nature communications

Article

https://doi.org/10.1038/s41467-025-61260-9

Preserving high-pressure solids via freestanding thin-film engineering

Received: 18 February 2025

Accepted: 18 June 2025

Published online: 01 July 2025

Check for updates

Tao Liang[1,2], Zhidan Zeng[1] ✉, Ziyin Yang[3,4], Fujun Lan[1,2,5], Hongbo Lou[1,5], Chendi Yang[6], Di Peng[5], Yuxin Liu[1], Tao Luo[1], Zhenfang Xing[1], Qing Wang[7], Haibo Ke[4], Yong Yang[3,8] ✉, Renchao Che[6] ✉, Hongwei Sheng[9], Ho-kwang Mao[1,5] & Qiaoshi Zeng[1,5] ✉

High pressure can significantly alter atomic and electronic structures of materials, resulting in unique properties. However, pressure-induced changes are often reversible, limiting their fundamental research and practical applications under ambient conditions. Here, we introduce a general method to preserve high-pressure solids under ambient conditions. By using freestanding carbon-gold-nanoparticle-carbon sandwiched thin films as precursors, we synthesize nanostructured diamond capsules that encapsulate high-pressure gold via an amorphous carbon-to-diamond transition. The preserved pressure is demonstrated to be tunable, ranging from 15.6 to 26.2 GPa, as the synthesis pressure increases from 32.0 to 56.0 GPa. This study establishes a scalable method to preserve high-pressure solids with controllable particle size and distribution through thin film engineering. Moreover, it enables in situ characterization of high-pressure solids with high spatial resolution at the atomic scale using electron beams, as well as other general diagnostic probes, and provides a viable route for large-scale applications of high-pressure solids.

High pressure induces significant changes in the structure and properties of materials[1,2]. Recent advances in high-pressure devices and in situ characterization techniques have opened new frontiers in materials exploration that were otherwise inaccessible under ambient conditions, including breakthroughs in high-temperature superconductivity[3–5], metallic hydrogen[6], exotic chemical compounds[7,8], and high-energy density materials[9,10]. However, the structure and property changes induced by high pressure are typically reversible and exist only within the contained environment of bulky high-pressure devices, hindering the applicability of high-pressure materials under ambient conditions. Additionally, while advanced in situ techniques have been developed to study the atomic and electronic structures of high-pressure materials[11], methods with low penetration depth, such as electron microscopy, are incompatible with traditional high-pressure devices like diamond-anvil cells (DACs) and large volume presses. These limitations prevent most high-pressure materials from being investigated in detail with atomic-scale spatial resolution, which is a hallmark of modern materials research.

A recent study aiming to address these long-standing challenges developed nanostructured diamond capsules (NDCs) through sp^2-bonded carbon to sp^3-bonded diamond transition, enabling the preservation of high-pressure materials and their characterization using

[1]Center for High Pressure Science and Technology Advanced Research, Shanghai, China. [2]Shanghai Institute of Laser Plasma, Shanghai, China. [3]Department of Mechanical Engineering, College of Engineering, City University of Hong Kong, Kowloon, Hong Kong, China. [4]Songshan Lake Materials Laboratory, Dongguan, China. [5]Shanghai Key Laboratory of Material Frontiers Research in Extreme Environments (MFree), Shanghai Advanced Research in Physical Sciences (SHARPS), Shanghai, China. [6]Laboratory of Advanced Materials, Shanghai Key Lab of Molecular Catalysis and Innovative Materials, Advanced Coatings Research Center of Ministry of Education of China, Sate Key Laboratory of Coatings for Advanced Equipment, Fudan University, Shanghai, China. [7]Laboratory for Microstructures, Institute of Materials, Shanghai University, Shanghai, China. [8]Department of Materials Science and Engineering, College of Engineering, City University of Hong Kong, Kowloon, Hong Kong, China. [9]Department of Physics and Astronomy, George Mason University, Fairfax, VA, USA. ✉e-mail: zengzd@hpstar.ac.cn; yonyang@cityu.edu.hk; rcche@fudan.edu.cn; zengqs@hpstar.ac.cn

various diagnostic probes at ambient conditions[12]. The synthesis process of NDCs is quite similar to the formation process of natural diamond inclusions, such as ice-VII, δ- N_2, etc[13–15]. Specifically, using glassy carbon with enclosed nanopores as a precursor, high-pressure volatiles, demonstrated using argon and neon, first diffuse into the nanopores of glassy carbon driven by pressure inside a DAC. These volatiles are then permanently sealed within the NDCs at target pressures after the glassy carbon-to-diamond transition upon heating. Once the external pressure is released and the high-pressure device (DAC) is removed, the volatiles remain at high pressure within the freestanding NDCs in ambient environments. Additionally, as composite materials containing high-pressure nano-inclusions, NDCs enable in situ high-pressure characterization using vacuum-based techniques, such as transmission electron microscopy (TEM), which are otherwise incompatible with traditional high-pressure setups[12]. However, this method is restricted to volatiles by the diffusion mechanism; therefore, it cannot be applied to solids.

High-energy electron radiation has been used to generate pressure within nanoparticles encapsulated in nanostructured carbon by knocking out outer-layer carbon atoms[16–18]. However, this method is limited to individual nanoparticles studied via TEM, making it impractical for large-scale material synthesis. A recent follow-up study expanded the NDCs concept by synthesizing bulk diamonds in a large-volume press. These bulk diamonds encapsulated Pt or Bi foil (with a thickness of ~20 μm and a lateral dimension of ~2 mm) were shown to maintain pressures up to ~3.5 GPa, as confirmed by x-ray diffraction (XRD)[19]. However, the resulting large and thick high-pressure solids are unsuitable for TEM studies, similar to the challenges typically encountered in studies on natural diamond inclusions[13]. In contrast, nanomaterials are naturally well-suited for atomic-scale TEM characterization. In principle, synthesizing NDCs through high-pressure and high-temperature (HPHT) treatment of carbon powders mixed with target nanopowder materials is feasible, as previously proposed[12]. However, it remains technically challenging because nanopowders tend to aggregate rather than stay homogeneously distributed in a solid powder mixture. Therefore, ensuring uniform separation and encapsulation of target nano-solids in the precursor is critical, yet challenging.

In this study, gold nanoparticles (AuNPs) were used as a demonstration material, and a multilayer thin film strategy was adopted to create freestanding carbon-gold-nanoparticles-carbon (C-AuNPs-C) sandwiched thin films as precursors. The thickness of the carbon layers, as well as the size and distribution of AuNPs, could be designed and readily controlled. Using HPHT treatment (illustrated in Fig. 1), freestanding NDCs containing well-dispersed high-pressure AuNPs were successfully synthesized, with pressures reaching up to ~26 GPa. Furthermore, the preserved pressure of the AuNPs could be adjusted by varying the synthesis pressures. This approach provides a versatile solution for preserving high-pressure solids at ambient conditions and enables direct in situ characterization of them with high spatial resolution techniques like TEM, overcoming previous limitations of traditional high-pressure devices in preserving and studying high-pressure solids.

Results and discussion

We fabricated freestanding C-AuNPs-C sandwiched thin films through the polymer-surface-buckling-enabled exfoliation method by sputtering carbon, gold, and carbon sequentially (see Experimental method for detailed description)[20,21]. The TEM image of the film cross-section (Fig. 2a) confirms that AuNPs are embedded between two adjacent carbon layers. No distinct interface is visible between the carbon layers, suggesting a dense monolithic structure. The carbon layers present an amorphous structure with mainly sp^2 bonding, as evidenced by electron energy loss spectroscopy (EELS) (Supplementary Fig. S1). Both the cross-sectional and plan-view TEM images (Fig. 2a, b) show that the AuNPs are well dispersed within the amorphous carbon film. Statistical analysis of ~100 AuNPs suggests that they have an average diameter of 6.1 ± 2.1 nm (Fig. 2c). The atomic structure of Au is well known to exhibit face-centered cubic (fcc) symmetry. According to the high-resolution TEM (HRTEM) image, the average interplanar spacing of Au (111) is 2.35 ± 0.01 Å in AuNPs (Fig. 2d), which is slightly smaller than that (2.36 Å) of bulk gold[22,23]. To evaluate the strain in AuNPs, the average interplanar spacing of Au (200) is also measured (2.03 ± 0.01 Å). The lattice parameters of AuNPs derived from the (111) and (200) d-spacings are nearly identical (a = 4.07 Å and 4.05 Å, respectively, with a difference less than the experimental uncertainty of ~1%), indicating that the strain in the AuNPs of the starting material is negligible.

To synthesize NDCs, the next step involves combining high pressure and high temperature to convert the sp^2-bonded amorphous carbon in the C-AuNPs-C films into diamond, thereby permanently encapsulating high-pressure AuNPs in diamond. Twenty layers of the C-AuNPs-C films were stacked and loaded into the sample chamber of a DAC for the HPHT treatment, as illustrated in Fig. 3a. The sample was compressed to ~56 GPa, then heated to ~2200 K using a double-sided laser heating system. Upon fully releasing the pressure of the DAC, the Raman spectrum of the HPHT-treated sample (Fig. 3b) suggests that the amorphous carbon was converted into diamond. The fragments of

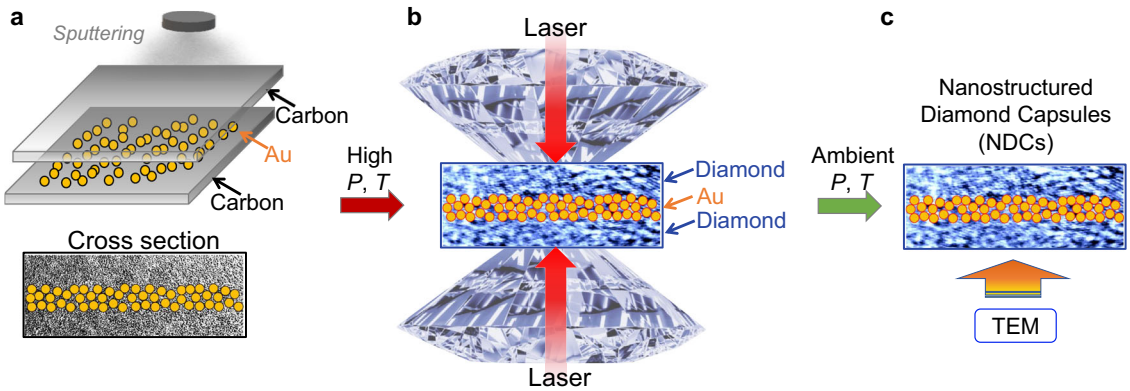

Fig. 1 | Schematic of the synthesis process of NDCs encapsulating high-pressure solids using multilayer thin film deposition. a Step 1: the C-AuNPs-C sandwiched film produced by magnetron sputtering contains dispersed Au nanoparticles. **b** Step 2: the multilayer carbon film is converted to nanocrystalline diamonds by in situ high-pressure laser heating in a DAC. **c** Step 3: the high-pressure Au nanoparticles are preserved in NDCs, which can be removed from the DAC and characterized by high-resolution TEM and various other probes. The diamond anvil cartoon is reproduced from ref. 12 with permission from Springer Nature.

https://doi.org/10.1038/s41467-025-61260-9

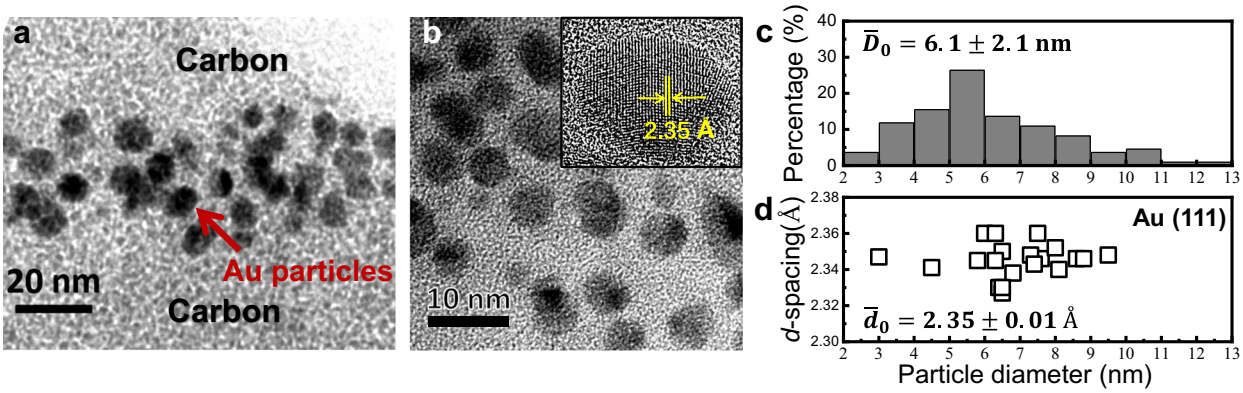

Fig. 2 | Characterization of C-AuNPs-C sandwiched thin film precursors. a A TEM image showing the cross-section of the C-AuNPs-C film with a total thickness of ~90 nm. The scale bar represents 20 nm. **b** A plan-view TEM image of the film showing the distribution of AuNPs. The scale bar represents 10 nm. The inset shows an HRTEM image of an AuNP with the (111) *d*-spacing of ~2.35 Å. **c** Size distribution of the AuNPs derived from ~100 nanoparticles from one sample. **d** (111) *d*-spacing of the analyzed AuNPs. The variation in Au (111) *d*-spacing is ~1%, which is mainly attributed to experimental uncertainty. The TEM studies on precursors were independently repeated twice, showing similar results.

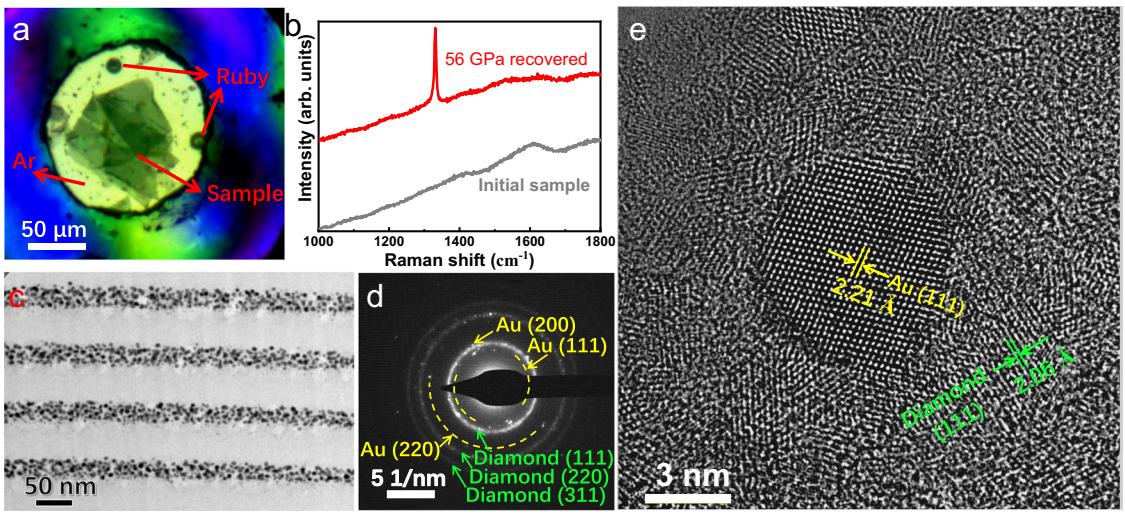

Fig. 3 | Synthesis and characterization of NDCs encapsulating high-pressure AuNPs using freestanding C-AuNPs-C films as precursors. a An optical microscopy image showing ~20 stacked layers of C-AuNPs-C films loaded into the sample chamber of a DAC. The scale bar represents 50 μm. **b** Raman spectra of the initial sample and the sample recovered from ~56 GPa and ~2200 K. **c** A TEM image of the cross-section of the sample recovered from ~56 GPa. **d** A SAED image of the sample, showing diffraction rings corresponding to an fcc Au and a cubic diamond phase. The scale bar represents 5 nm^{-1}. **e** An HRTEM image of an AuNP with (111) *d*-spacing of ~2.21 Å, surrounded by nanocrystalline diamonds with (111) *d*-spacing of ~2.06 Å. The scale bar represents 3 nm. The TEM studies on the sample treated under the same HPHT conditions were conducted on materials from a single synthesis experiment.

the sample were further analyzed using TEM. AuNPs remained uniformly distributed within the diamond matrix (see Fig. 3c), similar to the initial sample. The selected area electron diffraction (SAED) pattern can be indexed to an *fcc* Au phase plus a cubic diamond phase (Fig. 3d). Cross-sectional TEM images and SAED of the sample are consistent with the plan-view TEM results (Supplementary Fig. S2). The HRTEM image of an AuNP (Fig. 3e) shows the nanoparticle embedded in nanocrystalline diamonds with its (111) *d*-spacing of ~2.06 Å, consistent with the SAED results. The average (111) *d*-spacing of the AuNP is ~2.21 Å, significantly smaller than 2.35 Å observed in the initial C-AuNPs-C film sample, suggesting the AuNP is under substantial compressive stress (pressure) after the HPHT treatment. These TEM results demonstrate that we have successfully synthesized NDCs containing high-pressure AuNPs. In addition, it is interesting to note that the diamond interface region (~3–4 atomic layers adjacent to the high-pressure AuNP) is noticeably more disordered than regions further away. This observation suggests that NDCs provide a valuable opportunity to investigate the atomic-scale characteristics of extremely high-pressure interfaces, which are typically inaccessible through other characterization methods (Supplementary Fig. S3).

Furthermore, the size and lattice parameters of the encapsulated AuNPs were investigated over more particles to get statistical results. Figure 4a shows that these AuNPs have an average diameter of 6.5 ± 2.2 nm, slightly larger than that in the initial sample (6.1 ± 2.1 nm). Given the limited number of particles included in the HRTEM measurement, the wide size distribution, and potential errors arising from imperfect particle roundness, the observed variation of 0.4 nm (well within the measurement error of ~2 nm) in average particle size is not statistically significant. Figure 4b shows the Au (111) *d*-spacing of these AuNPs, with the data from the initial AuNPs (d_0) for comparison. The

https://doi.org/10.1038/s41467-025-61260-9

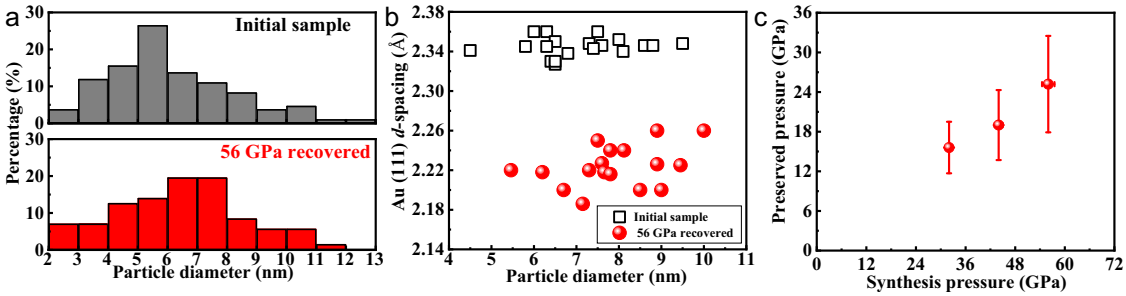

Fig. 4 | Estimation of preserved pressures in AuNPs encapsulated in NDCs. Comparison of the size distribution and average diameter, $\bar{D}$, (**a**) and (111) *d*-spacing of the AuNPs (**b**) between the initial sample and the sample recovered from the 56 GPa–2200 K treatment. Each data point in **b** represents the *d*-spacing determined by TEM on an individual AuNP. **c** Preserved pressure of AuNPs as a function of NDCs synthesis pressure. The preserved pressures are presented as mean values ±SD. The error bars are calculated based on *d* spacing, they are relatively large due to the fluctuation in *d*-spacing estimation across individual AuNPs by HRTEM. The error bars for the synthesis pressure represent the pressure gradient in the pressure-transmitting medium, argon.

average (111) *d*-spacing of the AuNPs decreases by ~5.5%, from 2.35 ± 0.01 Å in the initial sample to 2.22 ± 0.02 Å in NDCs. Since these AuNPs remain nearly spherical (no obvious shear deformation) and fully embedded in nanocrystalline diamonds, they are likely under quasi-hydrostatic compression. Therefore, the pressure in these AuNPs can be determined based on their lattice parameter and the equation of state (EOS) of bulk Au[24,25], which yields an estimated pressure of ~48 GPa in these AuNPs.

Since the behavior of AuNPs may differ from their bulk counterparts, the pressure preserved in the AuNPs may deviate from the estimation using the EOS of bulk Au. Due to discrepancies in the EOS of AuNPs reported in previous studies[22,26], we performed in situ high-pressure XRD on our initial C-AuNPs-C sample to determine the EOS of our AuNPs (Supplementary Fig. S4). The results suggest that our AuNPs have a bulk modulus of ~163 GPa, only slightly lower than that of bulk Au (167 GPa). In addition, although carbon has negligible solubility in bulk Au, previous studies have shown that a minimal amount of carbon atoms may diffuse into AuNPs and partially occupy octahedral interstitial or substitutional sites in the *fcc* structure, leading to slight lattice contraction[27,28]. To separate various possible effects induced by HPHT treatment from the preserved pressure effect on the AuNP lattice parameter, we conducted two additional HPHT experiments at ~5.5 GPa, ~2200 K and ~10 GPa, ~2200 K (Supplementary Fig. S5). These conditions are below the pressure required for the sp^2-bonded carbon to diamond transition[29] and therefore, they do not preserve high remnant pressures within the AuNP grains. The nearly identical *d*-spacing of AuNPs retrieved from these two HPHT experiments indicates the absence of a pronounced pressure effect on carbon solubility, but indicates only a temperature effect. Therefore, the recovered AuNPs (111) *d*-spacing (2.31 ± 0.02 Å) from the ~5.5 GPa or ~10 GPa and ~2200 K treatment can be used as a reference to calibrate the zero-pressure lattice of AuNPs after high temperature treatment. The slightly smaller *d*-spacing might include the contribution of the high-temperature enhanced solubility of carbon in AuNPs, which leads to lattice shrinkage. After this zero-pressure lattice correction, the pressure of the AuNPs in the NDCs synthesized at ~56 GPa is re-estimated to be ~26.2 GPa.

Furthermore, it is demonstrated by additional experiments (Supplementary Figs. S6 and S7) that the pressure preserved in AuNPs within NDCs can be tuned by regulating the synthesis pressure of NDCs. Fig. 4c shows the preserved pressure in AuNPs as a function of the synthesis pressures. The preserved pressure primarily arises from differences in compressibility between diamond and Au. During decompression from the synthesis pressure of NDCs, the volume expansion of encapsulated AuNPs is constrained by the extremely rigid diamond capsule, resulting in partial retention of the synthesis pressure in AuNPs after external pressure release. Therefore, the preserved pressure increases with increasing synthesis pressure, similar to the case in natural diamond inclusions, where higher preserved pressure also reflects higher formation pressures (formation depth of the natural diamonds)[30]. A similar relaxation of pressure by 2–3 GPa was previously observed during sample thinning of natural diamonds with high pressure inclusions[14,15]. Therefore, it should be noted that the relatively large uncertainty in preserved pressures (as also reflected by the variations in *d*-spacing in Fig. 4b) may also be related to the pressure relaxation in the extremely thin TEM sample after mechanically crushing or cutting using focused ion beam (FIB). It is not likely caused by a significant global pressure gradient in the NDC sample, given the good hydrostaticity of Ar as the pressure medium at high temperatures. Specifically, the AuNPs that are very close to the TEM sample surface may relax because the surface diamond layer is too thin to sustain extremely high pressure. In addition, the preservation of high-pressure AuNPs highly depends on the effective encapsulation by diamond. The pressure in AuNPs can be much lower or even close to ambient pressure if the surrounding amorphous carbon does not fully transform into diamond. This situation could occur in regions of the sample where laser heating does not reach the target temperature due to poor sample-laser coupling. Despite the rough estimation with relatively large errors, Fig. 4c shows that the average preserved pressure in AuNPs increases nearly in a linear manner from 15.6 to 26.2 GPa when the synthesis pressure is raised from 32.0 to 56.0 GPa. This near-linear relationship is consistent with the previous observation in NDCs with volatiles[12] and also suggests the effective encapsulation of high-pressure solids using this thin film engineering strategy.

In summary, we present a general strategy to preserve high-pressure solids using NDCs. As a demonstration, we synthesized NDCs containing AuNPs at pressures up to ~26 GPa using freestanding C-AuNPs-C sandwiched films as precursors. The pressure preserved in the AuNPs can be adjusted by controlling the synthesis pressure of the NDCs, following a nearly linear relationship up to tens of GPa. The NDCs allow for in situ investigation with high spatial resolution at the atomic scale, including morphology, composition, and structure (defects) in high-pressure solids using HRTEM. Combining such TEM with additional powerful characterization techniques, comprehensive studies could be carried out on high-pressure solids, which were previously only feasible for ambient condition samples. Moreover, in this work, the size and distribution of the initial AuNPs, which can be well-controlled in the film fabrication process, are largely maintained in the NDCs. This enables the synthesis of high-pressure AuNPs with designated pressures, particle sizes, and spatial distributions. This method can be extended to various other solids, helping enhance our understanding of their structures and properties under high pressure. In addition, nanomaterials often exhibit extraordinary optical, electronic, optoelectronic, and magnetic properties under pressure[31–34]. The transparency of the diamond capsules offers a unique opportunity for

the application of high-pressure nanomaterials, particularly those with extraordinary optical and magnetic properties.

Methods

Fabrication of sandwiched C-AuNPs-C films

Carbon films and AuNPs were deposited onto a polyvinyl alcohol hydrogel substrate by magnetron sputtering using high-purity carbon (99.99 wt.%) and gold (99.99 wt.%) targets. A carbon layer was deposited for 3900 s with a radio frequency power of 200 W. Then, AuNPs were deposited by sputtering for 9 s, followed by deposition of another layer of carbon for 3900 s. The deposition was conducted under the argon pressure of 20 mTorr with an argon flow rate of 30 sccm. The thickness of this C-AuNPs-C sandwiched film was ~90 nm as measured by atomic force microscopy. The fabricated sandwiched film could be exfoliated completely from the polyvinyl alcohol hydrogel substrate by immersing the sample in deionized water.

In situ high-pressure laser heating experiments

Approximately 20 layers of C-AuNPs-C films were stacked, cut into a square with an appropriate size, and loaded into a symmetric DAC with a culet size of around 300 μm. The DAC sample chamber was an ~150-μm-diameter hole drilled in a pre-indented rhenium gasket, and the sample was placed in the center of the chamber with tiny ruby balls loaded along as pressure calibrants. High-purity argon was loaded into the chamber using a gas-loading system, serving as both the pressure-transmitting and thermal-insulating medium. After gas loading, the sample was compressed to the target pressures and then heated to ~2200 K using a double-sided infrared laser heating system (wavelength 1064 nm)[35]. The temperature was determined by fitting the thermal radiation spectra of the heated sample to the Planck radiation function in a specific wavelength range.

Raman spectroscopy and TEM experiments

Raman spectra of the initial and recovered samples were acquired with the Renishaw inVia Raman microscope equipped with a 532 nm excitation laser. The TEM samples were prepared by mechanically crushing the synthesized NDC sample or using a FEI Versa 3D dual-beam FIB. The copper grid with lacey carbon (crashed samples) and copper holder (FIB processed samples) were used as the sample supports. HRTEM images and SAED patterns were collected using a FEI Tecnai F20 microscope operated at 200 kV. Additional spherical aberration-corrected HRTEM images of nanocrystalline diamond and AuNPs were collected using a Spectra 300 field emission TEM operated at 300 kV. The lattice spacing in the HRTEM images was measured using the software DigitalMicrograph by averaging interplanar spacing over multiple lattice planes. The carbon *K*-edge EELS measurement was conducted using a FEI Titan3 Themis G3 60–300 electron microscope operated at 300 kV, and the energy resolution is 0.15 eV.

In situ high-pressure XRD

In situ high-pressure XRD experiments were performed using a diffractometer equipped with an In-Ga target (MetalJet E1 + 160 kV). The X-ray wavelength was 0.5124 Å, and the beam size was ~100 × 100 μm^2. About 70 layers of C-AuNPs-C sandwiched films were stacked and loaded into a symmetric DAC with a culet size of ~400 μm. The DAC sample chamber was a ~270-μm-diameter hole drilled in a pre-indented rhenium gasket. Methanol-ethanol mixture (volume ratio of 4:1) was used as the hydrostatic pressure-transmitting medium below 10 GPa[36]. Tiny ruby balls were loaded in the sample chamber of the DAC for pressure calibration. Two-dimensional diffraction images were collected using an area detector (PILATUS R CdTe 1 M) and integrated into one-dimensional XRD patterns using the software Dioptas[37]. The diffraction peaks were fitted using the software Peakfit, and the EOS was fitted using the software EOSFit[38].

Data availability

The data that supporting the findings of this research are available within the article and its Supplementary Information. Source data are provided with this paper.

References

1. Mao, H.-K., Chen, X.-J., Ding, Y., Li, B. & Wang, L. Solids, liquids, and gases under high pressure. *Rev. Mod. Phys.* **90**, 015007 (2018).
2. Yoo, C.-S. Chemistry under extreme conditions: pressure evolution of chemical bonding and structure in dense solids. *Matter Radiat. Extrem.* **5**, 018202 (2020).
3. Zhu, Y. et al. Superconductivity in pressurized trilayer La4Ni3O10–δ single crystals. *Nature* **631**, 531–536 (2024).
4. Drozdov, A. P., Eremets, M. I., Troyan, I. A., Ksenofontov, V. & Shylin, S. I. Conventional superconductivity at 203 kelvin at high pressures in the sulfur hydride system. *Nature* **525**, 73 (2015).
5. Sun, H. et al. Signatures of superconductivity near 80 K in a nickelate under high pressure. *Nature* **621**, 493–498 (2023).
6. Loubeyre, P., Occelli, F. & Dumas, P. Synchrotron infrared spectroscopic evidence of the probable transition to metal hydrogen. *Nature* **577**, 631–635 (2020).
7. Zhang, W. et al. Unexpected stable stoichiometries of sodium chlorides. *Science* **342**, 1502–1505 (2012).
8. Dong, X. et al. A stable compound of helium and sodium at high pressure. *Nat. Chem.* **9**, 440–445 (2017).
9. Ji, C. et al. Nitrogen in black phosphorus structure. *Sci. Adv.* **6**, eaba9206 (2020).
10. Laniel, D. et al. High-pressure polymeric nitrogen allotrope with the black phosphorus structure. *Phys. Rev. Lett.* **124**, 216001 (2020).
11. Mao, H.-K. et al. Recent advances in high-pressure science and technology. *Matter Radiat. Extrem.* **1**, 59–75 (2016).
12. Zeng, Z. et al. Preservation of high-pressure volatiles in nanostructured diamond capsules. *Nature* **608**, 513–517 (2022).
13. Tschauner, O. et al. Ice-VII inclusions in diamonds: evidence for aqueous fluid in Earth's deep mantle. *Science* **359**, 1136–1139 (2018).
14. Navon, O. et al. Solid molecular nitrogen (δ-N2) inclusions in Juina diamonds: exsolution at the base of the transition zone. *Earth Planet. Sci. Lett.* **464**, 237–247 (2017).
15. Tschauner, O. et al. Long-term relaxation of orientational disorder and structural modifications in molecular nitrogen at high pressure. *J. Chem. Phys.* **161**, 204506 (2024).
16. Wu, J. & Buseck, P. R. In-situ high-pressure transmission electron microscopy for Earth and materials sciences. *Am. Mineral.* **99**, 1521–1527 (2014).
17. Sun, L., Banhart, F., Krasheninnikov, A. V., Rodríguez-Manzo, J. A., Terrones, M. & Ajayan, P. M. Carbon nanotubes as high-pressure cylinders and nanoextruders. *Science* **312**, 1199–1202 (2006).
18. Wang, Z. & Zhao, Y. High-pressure microscopy. *Science* **312**, 1149–1150 (2006).
19. Tang, Y., Wu, J., Dong, H., Ouyang, X. & Wang, H. Preserving a large-scale reversible high-pressure phase under ambient conditions. *Mater. Res. Lett.* **12**, 132–139 (2024).
20. Yu, Q. et al. Transformation of freestanding carbon-containing gold nanosheets into Au nanoparticles encapsulated within amorphous carbon: implications for surface modification of complex-shaped materials and structures. *ACS Appl. Nano Mater.* **4**, 5098–5105 (2021).
21. Wang, T. et al. The controlled large-area synthesis of two dimensional metals. *Mater. Today* **36**, 30–39 (2020).
22. Yu, X., Rong, J., Zhan, Z., Liu, Z. & Liu, J. Effects of grain size and thermodynamic energy on the lattice parameters of metallic nanomaterials. *Mater. Des.* **83**, 159–163 (2015).

23. Takemura, K. Evaluation of the hydrostaticity of a helium-pressure medium with powder x-ray diffraction techniques. *J. Appl. Phys.* **89**, 662–668 (2001).
24. Anderson, O. L., Isaak, D. G. & Yamamoto, S. Anharmonicity and the equation of state for gold. *J. Appl. Phys.* **65**, 1534–1543 (1989).
25. Shim, S.-H. & Duffy, T. S. Kenichi T. Equation of state of gold and its application to the phase boundaries near 660 km depth in Earth's mantle. *Earth Planet. Sci. Lett.* **203**, 729–739 (2002).
26. Gu, Q. F., Krauss, G., Steurer, W., Gramm, F. & Cervellino, A. Unexpected high stiffness of Ag and Au nanoparticles. *Phys. Rev. Lett.* **100**, 045502 (2008).
27. Yu, Q. et al. Strong, ductile, and tough nanocrystal-assembled freestanding gold nanosheets. *Nano Lett.* **22**, 822–829 (2022).
28. Sutter, E. A. & Sutter, P. W. Giant carbon solubility in Au nanoparticles. *J. Mater. Sci.* **46**, 7090–7097 (2011).
29. Sundqvist, B. Carbon under pressure. *Phys. Rep.* **909**, 1–73 (2021).
30. Angel, R. J., Mazzucchelli, M. L., Alvaro, M., Nimis, P. & Nestola, F. Geobarometry from host-inclusion systems: the role of elastic relaxation. *Am. Mineral.* **99**, 2146–2149 (2014).
31. San-Miguel, A. Nanomaterials under high-pressure. *Chem. Soc. Rev.* **35**, 876–889 (2006).
32. Ma, Z. et al. Pressure-induced emission of cesium lead halide perovskite nanocrystals. *Nat. Commun.* **9**, 4506 (2018).
33. Yue L. et al. Radical n–p conduction switching and significant photoconductivity enhancement in NbOI 2 via pressure-modulated peierls distortion. *J. Am. Chem. Soc.* **146**, 25245–25252 (2024).
34. Lu, X. et al. Enhanced electron transport in Nb-doped TiO2 nanoparticles via pressure-induced phase transitions. *J. Am. Chem. Soc.* **136**, 419–426 (2014).
35. Zeng, Z. et al. Synthesis of quenchable amorphous diamond. *Nat. Commun.* **8**, 322 (2017).
36. Chen, X. et al. Structural transitions of 4:1 methanol–ethanol mixture and silicone oil under high pressure. *Matter Radiat. Extrem.* **6**, 038402 (2021).
37. Prescher, C. & Prakapenka, V. B. DIOPTAS: a program for reduction of two-dimensional X-ray diffraction data and data exploration. *High. Press. Res.* **35**, 223–230 (2015).
38. Gonzalez-Platas, J., Alvaro, M., Nestola, F. & Angel, R. EosFit7-GUI: a new graphical user interface for equation of state calculations, analyses and teaching. *J. Appl. Crystallogr.* **49**, 1377–1382 (2016).

Acknowledgements

The authors thank Yanping Yang, Xueyan Du, and Haiyun Shu from HPSTAR for their kind help with the experiments. The authors acknowledge the financial support from the National Key R&D Program of China (2021YFA0718900), Shanghai Science and Technology Committee, China (no. 22JC1410300), and Shanghai Key Laboratory of Material Frontiers Research in Extreme Environments, China (no. 22dz2260800). Y.Y. acknowledges the financial support provided by Research Grants Council, the Hong Kong Government, through the RGC-NSFC joint research scheme (N_CityU 109/21).

Author contributions

Q.S.Z. and Z.D.Z. initiated the project. H.K.M. supervised the project. Q.S.Z., Z.D.Z., Y.Y., and R.C.C. designed the experiments. T. Liang., Z.Y.Y., F.J.L., H.B.L., C.D.Y., D.P., Y.X.L., T.Luo., Z.F.X., Q.W., H.B.K., H.W.S., Z.D.Z., and Q.S.Z. performed the experiments and analyzed the data. T. Liang, Z.D.Z., and Q.S.Z. wrote the paper. All authors interpreted the results and commented on the manuscript.

Competing interests

Q.Z., Z.Z., T. Liang, Y.Y., and H.M. are in the process of applying for a patent (application no. CN202410821681.1 in China) related to the synthesis of NDCs for high-pressure solids described in this work. The other authors declare no competing interests.

Additional information

Supplementary information The online version contains supplementary material available at https://doi.org/10.1038/s41467-025-61260-9.

Correspondence and requests for materials should be addressed to Zhidan Zeng, Yong Yang, Renchao Che or Qiaoshi Zeng.

Peer review information *Nature Communications* thanks Hao Yan and the other, anonymous, reviewer(s) for their contribution to the peer review of this work. A peer review file is available.